Biochimica et Biophysica Acta, 648 (1981) 28–48
Elsevier/North-Holland Biomedical Press

BBA 79396

EVIDENCE FOR COOPERATIVE EFFECTS IN THE BINDING OF POLYVALENT METAL IONS TO PURE PHOSPHATIDYLCHOLINE BILAYER VESICLE SURFACES *

ADELA CHRZESZCZYK, ARNOLD WISHNIA and CHARLES S. SPRINGER, Jr.

Department of Chemistry, State University of New York at Stony Brook, Stony Brook, NY 11794 (U.S.A.)

(Received March 23rd, 1981)

Key words: Phospholipid bilayer; Phosphatidylcholine; Polyvalent metal ion; Cooperative binding; NMR

An internal NMR monitor for the study of lanthanide ion (Ln^{3+}) binding to phospholipid bilayer membranes has been developed. The dimethylphosphate anion, DMP^-, forms labile complexes with Ln^{3+} in aqueous solution and in solutions also containing bilayer dispersions. The hyperfine shift in the DMP^- resonance induced by Pr^{3+} ions has been used to determine the overall thermodynamic formation constants for the $Pr(DMP)^{2+}$ and $Pr(DMP)_2^+$ complexes: 81 (M^{-1}) and 349 (M^{-2}) at 52°C; the limiting hyperfine shift (^{31}P) at 52°C is 91.5 ppm downfield. These parameters, applied to the observed DMP^- hyperfine shift in the presence of the membrane, establish both the free Pr^{3+} concentration and the amount of Pr^{3+} bound to the phospholipid surface. Extensive data for the binding of Pr^{3+} to the outer surfaces of sonicated vesicles yield a limiting hyperfine shift per Pr^{3+} of 181.6 ppm downfield for the dipalmitoylphosphatidylcholine ^{31}P resonance at 52°C, clearly demonstrating that the binding stoichiometry is two DPPCs per Pr^{3+}. A Hill analysis indicates that the binding data are more anti-cooperative than a realistic Langmuir isotherm, yet more cooperative than a Stern isotherm incorporating electrostatic considerations at the Debye-Hückel level. Fittings to specific models lead to a cooperative model in which tense (T) sites, with low affinity for Pr^{3+}, present in the absence of metal ions, quickly give way to relaxed (R) sites (two DPPCs per site), with much higher affinity for Pr^{3+}, as the amount of Pr^{3+} bound to the surface increases. The intrinsic equilibrium constants for the binding of Pr^{3+} to DPPC vesicles are 2 M^{-1} and 3 000 M^{-1} for the T and R sites, respectively, at 52°C. The distribution coefficient between these sites ([R]/[T]) in the absence of Ln^{3+} is 0.14 at 52°C. We picture the binding site conversion as a head-group conformational change involving mostly the choline moiety. Sketchy results for binding on the inside vesicle surface indicate that the overall affinity for Pr^{3+} is significantly greater and suggest that the site stoichiometry may be different.

Introduction

Calcium binding is critical to many processes in protein, nucleic acid and membrane function. Lanthanide cations (Ln^{3+}) by reason of size and, to some extent, charge, are partial analogues, the spectroscopic properties of which make them useful investigative tools [1]. In particular, the equilibrium binding of Ln^{3+} ions to phospholipid bilayer surfaces has proven to be quite useful in NMR studies of a number of important membrane phenomena (for partial bibliographies, see Refs. 2–5). This is due to the fact that paramagnetic lanthanide ions induce a significant hyperfine shift in the positions of NMR lines of various magnetic nuclei in the phospholipid headgroup upon binding to the surface. As anticipated above, it is also now clear that Ln^{3+} ions do compete

* Taken, in part, from the Ph.D. Dissertation of A.C., State University of New York at Stony Brook, Stony Brook, December 1978; Presented, in part, in 'NMR in Macromolecules' symposium of the 21st Rocky Mountain Conference, Denver, CO, August 1979.

Abbreviations: DMP^-, dimethylphosphate anion; DPPC, dipalmitoylphosphatidylcholine.

0005-2736/81/0000–0000/$02.50

with Ca^{2+} ions in surface binding (Ref. 6 and Grandjean, J., unpublished data) probably occupying the same binding sites, and thus can be used to study biologically relevant Ca^{2+} binding.

There are a number of methods for measuring the binding of metal cations to macromolecules, polyelectrolytes or molecular aggregates. Among these are equilibrium dialysis, indicator competition, electrophoretic mobility and magnetic resonance techniques [7–9]. As might be expected in light of the above-mentioned hyperfine shift, a number of attempts to measure the binding of paramagnetic Ln^{3+} ions to phospholipid bilayers by NMR methods has been reported; the latest by Westman and Eriksson [10]. The authors of this report take great pains to extract the contact contribution to the observed hyperfine shift in the hope that it is not sensitive to the occurrence of a headgroup conformational change which is commonly thought to be triggered by initial Ln^{3+} binding. However, if the conformational change were actually to affect the nature of the binding equilibrium itself, then the observed contact contribution would almost certainly be also affected, and the normal NMR method is back in its typically underdetermined condition.

We have developed an NMR indicator method for bilayer systems [5] which avoids many a priori assumptions, and thereby specifically separates the actual determination of the Ln^{3+} binding isotherm from any hypothesis regarding the detailed process which gives the isotherm its functional form *. The indicator we have chosen is the dimethylphosphate anion (DMP^-), which ought to be a good analog for the phosphodiester binding site in phospholipid membranes and should have a quantitatively similar limiting ^{31}P hyperfine shift on binding Pr^{3+}. This shift is also the most likely to be dominated by intramolecular Pr^{3+} binding compared to that of any other common magnetic headgroup nucleus. The DMP^- anion should be a good competitor with the bilayer surface since simple phosphodiesters have long been used for organic solvent extractions of Ln^{3+} ions [11,12].

Fig. 1 depicts typical ^1H-decoupled and undecoupled ^{31}P spectra of aqueous NaDMP solutions of

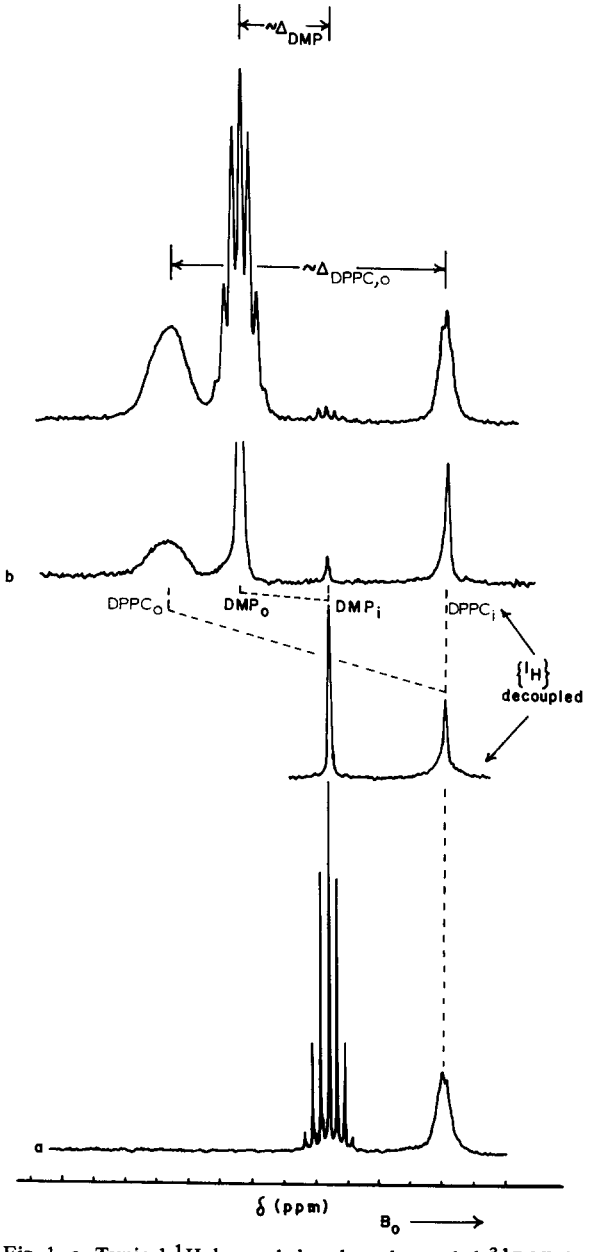

Fig. 1. a. Typical ^1H-decoupled and -undecoupled ^{31}P-NMR spectra of a solution of DPPC vesicles and sodium dimethylphosphate. ($T = 52°C$) b. The same solution with $Pr(NO_3)_3$ added to the outer aqueous volume. ($T = 52°C$, see Table II for typical concentrations.)

* An application of the NMR indicator approach has been reported [6], but using a relatively poor indicator, inadequate allowance for effects of ionic strength on the Ln^{3+} indicator equilibria, and a fundamentally incorrect expression for the Ln^{3+} vesicle surface binding isotherm which also begs the question of the true binding stoichiometry.

the DPPC vesicles above the phase transition temperature in the absence and presence of Pr^{3+} in the outer aqueous volume. The Ln^{3+} binding to the DMP^- anion and the outer surface is fast on the NMR timescale and thus the ^{31}P resonances of DPPC and DMP^- accessible to Pr^{3+} suffer a downfield hyperfine shift which depends on the amount of Pr^{3+} present. The resonances of the DPPC molecules on the inner vesicular surfaces and the DMP^- anions trapped in the inner aqueous volumes are not significantly shifted because the Pr^{3+} ions cannot penetrate to the inside of the vesicles. The observed values of the hyperfine shifts, Δ_{obs}, measured from the unshifted inner resonances, are defined in Fig. 1.

The parameters of the binding equilibria for DMP^- and Pr^{3+} can be determined quite accurately in separate solutions (see below). The observed change in the ^{31}P chemical shift of DMP^- in the presence of Pr^{3+} and membrane can then be used to determine the concentrations of free Pr^{3+} and Pr^{3+} bound to DMP^-. Since the total concentration of Pr^{3+} added is known, the concentration of Pr^{3+} bound to the phospholipid vesicles is determined independent of any hypotheses regarding the stoichiometry or magnetic properties of the Pr^{3+} phospholipid complexes.

Experimental

Materials

Synthetic L-α-dipalmitoylphosphatidylcholine was obtained from Sigma Chemical Co. at 98% purity and normally used without further purification. In the case of one lot, however, the NMR spectral resonances were broadened, implying that some paramagnetic impurities must be present. These solutions were therefore treated with Chelex 100 (Bio-Rad, 100–200 mesh, sodium form) before proceeding with the experiments. The $Pr(NO_3)_3$ used was a product of Alfa/Ventron and had a purity of 99.9%. Stock solutions of $Pr(NO_3)_3$ were prepared in ^2H_2O (either Bio-Rad, 99.85 mol% ^2H_2O, or Merck, 99.7 atom% ^2H) and the Pr^{3+} concentration was determined by cation exchange on proton loaded Dowex 50W-X8 exchange resin (Bio-Rad, 50–100 mesh, hydrogen form) followed by titration of the released protons.

Preparation of sodium dimethylphosphate

The method of preparation is based on a procedure for dealkylation of triesters of phosphoric acid [13]. Trimethylphosphate (Aldrich) and dried sodium iodide were added in equimolar quantities to acetone which had been dried over molecular sieves (Fisher Sci. Co., type 4A). The solution was stirred overnight at room temperature. The sodium salt of the diester precipitated and was washed with acetone. It was then dried under vacuum in the presence of an acetone/solid CO_2 trap. Both ^{31}P- and ^1H-NMR gave the expected spectra with no resonances representing impurities.

Vesicle preparation

Small, bilayer vesicles were formed by ultrasonication with a Branson W185 sonifier using a titanium microprobe tip. Typical solutions were prepared by adding the $NaDMP/^2H_2O$ stock solution to a nitrogen purged glass vessel, maintained by an outer water jacket at 52°C. An appropriate quantity of DPPC, of the order of 200 mg/2 ml, was added to the salt solution. Nitrogen was bubbled through the solution for 10–15 min via a long syringe needle, gently, to prevent 'sudsing'. Thereupon, the solution was sonicated for 25–30 min at a power output of 40–50 W, nitrogen continually passing over the top of the solution. A nearly translucent solution was obtained. Three 10–15 μl samples were then removed for phosphate analysis. The vesicle solution was then centrifuged in a capped plastic tube for 10 min at approx. 42°C using a Sorvall RC2-B centrifuge operating at 10 000 rev./min (approx. 12 000 × *g*). The centrifugation sediments any titanium and buoys excess aggregated lipid. The clear solution containing small vesicles was then withdrawn carefully from below the fluffy aggregate with a syringe, total volume being noted, and transferred to a nitrogen-purged 10 mm NMR tube. Three 10–15 μl samples were again taken for phosphate anlayses. At the end of the NMR experiment, phosphate analysis of the vesicle solution and the NaDMP stock solution were also carried out.

Phosphate analyses

The method of Chen et al. [14] was used to determine phosphate concentrations. In our hands, the phosphomolybdate complexes produced from National Bureau of Standards KH_2PO_4 or Na_2HPO_4 gave apparent absorptivities of $2.57 \cdot 10^4$ $M^{-1} \cdot cm^{-1}$ at 620 nm (Cary 14 spectrophotometer). The spread in triplicate analyses of a phospholipid solution was less than 5% in most cases.

NMR sample preparation

Aliquots of analyzed concentrated stock $Pr(NO_3)_3$ in ^2H_2O (0.3–0.4 M) were added to known volumes of analyzed NaDMP or DPPC-vesicle/NaDMP solutions in ^2H_2O. Additivity of volumes was assumed. For the studies of Pr^{3+} binding to the outer monolayer of the DPPC vesicle (the main emphasis of the present paper) the volume of the bilayer and of the intravesicular aqueous space was subtracted from the total volume in order to calculate the concentration (mol/l of external aqueous space) of Pr^{3+} and of outer DPPC (2/3 of the total DPPC [15]). For NaDMP, which is distributed throughout both the outside and inside aqueous volumes, only the lipid volume was subtracted.

For the few experiments involving Pr^{3+} binding to both the inner and outer monolayers of the bilayer, only the bilayer volume was subtracted from the total in order to calculate the concentrations; it is assumed that the free ion concentrations are the same inside and outside the vesicles after sonication to equilibrium.

It is also important to note that sufficient time be given for those samples to which $Pr(NO_3)_3$ is added to equilibrate completely in the NMR probe after each addition. They were allowed up to 20 min before data collection was commenced.

NMR spectroscopy

All ^{31}P-NMR experiments were carried out at 40.502 MHz on a Varian XL-100 spectrometer with 12-inch magnet (23.49 kG) and operating in the Fourier transform (FT) mode at 52.5 ± 0.5°C, unless otherwise noted. A Varian Data Machines 620/L-100 computer unit was utilized for all FT operations. The pulse width required for a 90° flip for ^{31}P, checked periodically, was found to range between 39 and 42 μs. Other FT parameters, including the number of transients, pulse delay, and acquisition time, varied somewhat; however, 'typical' ranges are: 500–1 000, 100–125 s and 3–8 s, respectively. The pulse delay can be considerably shortened by reducing the pulse width appropriately. Most measurements of resonance areas were done by planimetry; others by electronic integration on the NMR recorder.

All ^{1}H-NMR experiments were conducted on the same machine at 100 MHz, and employed standard NMR parameters.

Data reduction

All fittings were carried out on a UNIVAC 1 110 computer with a non-linear least-squares program developed for a variety of applications (see, for example, Ref. 16), with appropriate modifications for the various equilibrium models. In general, the subroutines calculate the free and bound concentrations of the species under consideration, for the current set of values of the parameters, by an iterative procedure, until mass conservation of all species is obtained. These are used in the least-squares algorithm to obtain corrections to the parameters, and the process continues until a best fit is obtained. The parameters are usually the limiting shift, Δ°, and the equilibrium constants. The calculated dependent variable may be either chemical shift (e.g., sodium dimethylphosphate-$Pr(NO_3)_3$ fittings) or the bound concentration of a given species (e.g, outer DPPC fittings). Further description of these subroutine variations will be brought out in the text.

Results

The Praseodymium(III) dimethylphosphate binding equilibria

As discussed above, the change in chemical shift of DMP^- is our prime indicator, to be used to determine not only the concentration of Pr^{3+} bound to DMP^- and the concentration of free Pr^{3+}, but also, by difference, the concentration of Pr^{3+} bound by DPPC. An accurate characterization of the Pr^{3+}/DMP^- binding equilibria is therefore crucial. An extensive study of these equilibria was undertaken at the main experimental temperature for DPPC, 52°C, over a very wide range of Pr^{3+} and DMP^- concentrations and Pr^{3+}/DMP^- ratios (77 points in all). One of the data sets is shown in Fig. 2, others are described in the figure caption of Fig. 3, and, in addition, less extensive sets were also obtained at 28, 44, and 58°C.

The smooth downfield shift of the single DMP^- resonance with increasing Pr^{3+} concentration in Fig. 2 confirms our expectation that exchange of DMP^- among free DMP^- and its possible Pr^{3+} complexes is fast on the NMR timescale.

A priori, one had to assume that three complexes might be present: $Pr(DMP)^{2+}$, $Pr(DMP)_2^+$, $Pr(DMP)_3$, with formation constants K_1, K_2 and K_3. For conditions of rapid exchange, the NMR observation equa-

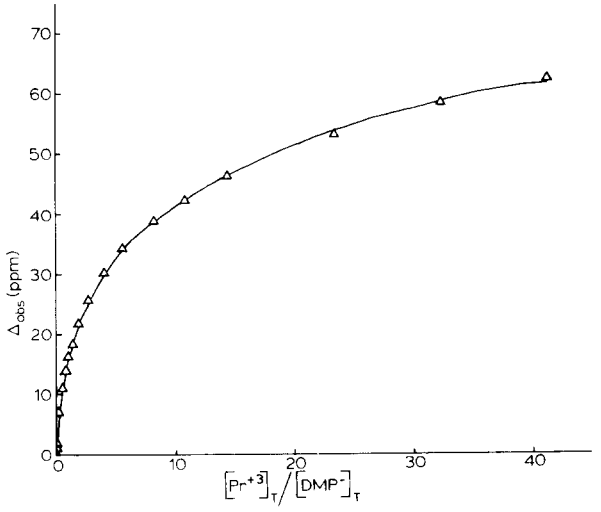

Fig. 2. The observed downfield isotropic hyperfine shift of the DMP^- ^{31}P-NMR signal with increasing $[Pr^{3+}]_T/[DMP^-]_T$ values, in ^2H_2O at 52°C. This data set ranged between the following stoichiometric molar concentrations of sodium dimethylphosphate : $Pr(NO_3)_3$; 0.00964 : 0.00029 (initial) to 0.00636 : 0.2627 (final). The triangles represent the experimental data while the solid curve represents a computer fitting to the data ($\mathring{a}$ held fixed at 6.20 Å, Δ° = 91.49 ppm, β_1 = 81.08, β_2 = 348.68, and β_3 = 0; see text).

tion is

$$\Delta_{obs} = (\Delta_1^\circ[ML^{2+}] + 2\Delta_2^\circ[ML_2^+] + 3\Delta_3^\circ[ML_3])/[L_T] \quad (1)$$

with concentrations given by the equilibria

$$Pr^{3+} + DMP^- = Pr(DMP)^{2+},$$

$$K_1 = \frac{[ML^{2+}]}{[M^{3+}][L^-]} \frac{\gamma_{2+}}{\gamma_{3+}\gamma_{1-}} \quad (2)$$

$$Pr(DMP)^{2+} + DMP^- = Pr(DMP)_2^+,$$

$$K_2 = \frac{[ML_2^+]}{[ML^{2+}][L^-]} \frac{\gamma_{1+}}{\gamma_{2+}\gamma_{1-}} \quad (3)$$

$$Pr(DMP)_2^+ + DMP^- = Pr(DMP)_3,$$

$$K_3 = \frac{[ML_3]}{[ML_2^+][L^-]} \frac{\gamma_0}{\gamma_{1+}\gamma_{1-}} \quad (4)$$

$$[L_T] = [L^-] + [ML^{2+}] + 2[ML_2^+] + 3[ML_3] \quad (5)$$

The bracket terms are the equilibrium concentrations and the γ_i the corresponding single-ion molal activity coefficients. The symbol Δ_{obs} is the observed isotropic hyperfine shift, the difference between the chemical shift of DMP^- in solution with Pr^{3+} and the standard shift in the absence of Pr^{3+}. The ^{31}P resonance was used mostly, but some ^1H data were also obtained. The symbols Δ_1°, Δ_2° and Δ_3° are the limiting hyperfine shifts of the pure mono-, bis- and trisDMP^--Pr^{3+} complexes.

At this point, the description of the monotonic curve of Fig. 2 would seem to require an inordinate number of parameters: the six terms Δ_1°, Δ_2°, Δ_3°, K_1, K_2 and K_3, and however many are needed to evaluate the unknown (so far), quite ionic-strength-dependent activity coefficients γ_{3+}, γ_{2+}, γ_{1+}, γ_{1-}. To make a long story short, fitting studies with a variety of options showed that many of the parameters make little or no contribution to the system, or are not independent, or can be obtained from other kinds of data. In fact, at most, four parameters needed to be evaluated: K_1, K_2, $\Delta_1^\circ = \Delta_2^\circ$, and $\mathring{a}$, a mean distance of closest approach in extended Debye-Hückel theory.

Indeed, it turned out that $\mathring{a}$, the fitting parameter, agreed perfectly with the literature value of $\mathring{a}$ for $PrCl_3$ obtained from recent careful isopiestic determinations of the mean activity of various lanthanide chlorides [17]; satisfactory estimates of the single-ion activity coefficients in Eqns. 2–4 could be obtained entirely from these data.

Because the activity coefficients of $LaCl_3$ and $PrCl_3$ are almost identical [17], and the substitution of NO_3^- produces only small differences at the higher ionic strengths [18] (see Fig. 3), a Debye-Hückel approach, in which species of like charge and similar size can be treated as equivalent, was appropriate. Activity coefficients of neutral species (H_2O, ML_3) were taken as unity; those of monoanions equated ($\gamma_{DMP^-} = \gamma_{NO_3^-}$). If Eqns. 2 and 3 are multiplied by unity in the forms (γ_L^2/γ_L^2) and (γ_L/γ_L), Eqns. 2–4 can be re-expressed in terms of the more or less observable mean activity coefficients γ_{mn} for salts $(M^{m+})_n(L^{n-})_m$.

$$K_1 = \beta_1 = \frac{[ML^{2+}]}{[M^{3+}][L^-]} \frac{\gamma_{21}^3}{\gamma_{31}^4} \quad (6)$$

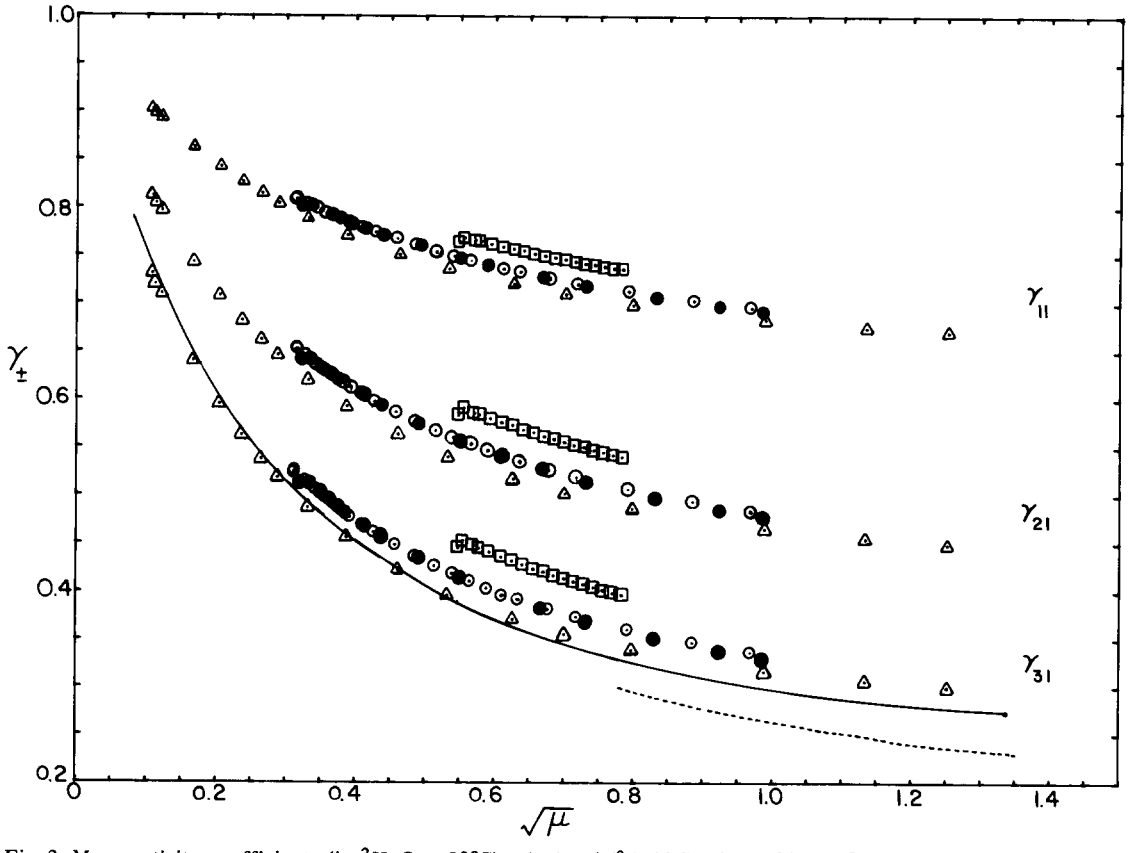

Fig. 3. Mean activity coefficients (in ^2H_2O at 52°C) calculated ($\hat{a}$ held fixed at 6.20 Å, Δ° = 91.49 ppm, β_1 = 81.08, β_2 = 348.68, and β_3 = 0) for $[Pr(DMP)_2]^+$ (upper set, γ_{11}), $[Pr(DMP)]^{2+}$ (middle set, γ_{21}) and Pr^{3+} (lower set, γ_{31}) as a function of the square root of the total ionic strength, $\sqrt{\mu}$. The solid curve represents experimental values for $LaCl_3$ and $PrCl_3$ at 25°C in H_2O [17]. The dashed curve represents experimental values for $La(NO_3)_3$ in H_2O at 25°C [18]. The symbols represent data sets with the following concentration ranges (given as molar concentrations of sodium dimethylphosphate: $Pr(NO_3)_3$, stoichiometric): △, 0.00964 : 0.00029 to 0.00636 : 0.2627 (the data set of Fig. 2); •, 0.09268 : 0.00262 to 0.05257 : 0.1677; ○, 0.0963 : 0.00029 to 0.0755 : 0.164; □, 0.288 : 0.00377 to 0.257 : 0.0981.

$$K_1K_2 = \beta_2 = \frac{[ML_2^+]}{[M^{3+}][L^-]^2}\frac{\gamma_{11}^2}{\gamma_{31}^4} \tag{7}$$

$$K_1K_2K_3 = \beta_3 = \frac{[ML_3]}{[M^{3+}][L^-]^3}\frac{1}{\gamma_{31}^4} \tag{8}$$

As usual,

$$\gamma_{31} \equiv (\gamma_{M^{3+}}\gamma_{L^-}^3)^{1/4} \tag{9}$$

$$\gamma_{21} \equiv (\gamma_{ML^{2+}}\gamma_{L^-}^2)^{1/3} \tag{10}$$

$$\gamma_{11} \equiv (\gamma_{ML_2^+}\gamma_{L^-})^{1/2} \tag{11}$$

The extended Debye-Hückel expression for γ_{mn}, generalized from Eqns. (3-4-6), (3-4-8a), (3-4-9), (3-5-8), (3-5-9) and (12-5-3) of Harned and Owen [19] is

$$\log \gamma_{mn} = \left\{\frac{-mn(1.290\cdot 10^6)(DT)^{-3/2}\sqrt{\Gamma}}{1 + 35.56(DT)^{-1/2}\,\hat{a}\,\sqrt{\Gamma}}\right\} - \log\left(1 + \sum_i \frac{\nu_i m_i}{55.5}\right) + D'\left(\sum_i c_i\right)^k \tag{12}$$

where D is the solvent dielectric constant, T the absolute temperature, ν_i the number of ions of salt i

(e.g., $m + n$ for M_nL_m), m_i and c_i the molal and molar concentrations, Γ the ional concentration (the sum over ionic concentrations $\Sigma_j c_j z_j^2$). The leading term is the modified Debye-Hückel limiting law expression: $\mathring{a}$, in Å, is formally the mean distance of closest approach of ions, and actually an omnium gatherum correction term for intermediate ionic strengths. The second term is the trivial conversion from rational mole-fraction activity coefficients $f_\pm$ to molal quantities $\gamma_\pm$. The third term, a standard arbitrary salting-out addition, is important only at high concentrations (by which point the predominant ions in our solutions are Pr^{3+} and NO_3^-).

The parameters D' (= 0.2168) and k (= 0.83) were evaluated from a least-squares fit of the 25°C $PrCl_3$ activity coefficient data [17]. It is assumed that these values hold with sufficient accuracy at other temperatures and in ^2H_2O. When the 52° Pr^{3+}-DMP^- binding data were subjected to four- or five-parameter fits, the values returned for $\mathring{a}$ clustered around 6.20 Å, in perfect agreement with the value of 6.175 Å obtained by Spedding and co-workers [17]. The values of γ_{31} agree very well with those of $PrCl_3$ and $Pr(NO_3)_3$ (note especially the triangles in Fig. 3), if one takes note of the differences in the DT factor due to temperature and deuteration of the solvent. The much less-ionic-strength-dependent values of γ_{11} and γ_{21} are very close to those of NaCl and $CaCl_2$ [19]. There may be a small systematic shift in $\mathring{a}$ with increasing concentrations of NaDMP (cf. Fig. 3). For the final fittings reported here, $\mathring{a}$ was fixed at the literature value, 6.2 Å, for all data sets. This value is also very reasonable in light of considerations of ionic radii.

We can now turn our attention to the shift parameters and the formation constants. It was immediately clear that the exclusive formation of a tris complex (Eqn. 8) was inconsistent with the data: the isotherms do not have that kind of curvature. When formation of all three complexes was permitted, the contribution of $[Pr(DMP)_3]$ was always negligible, and that of $Pr(DMP)_2^+$ almost always small (rarely even 20% of the Pr^{3+}-bound DMP^-). It is justified a posteriori, but with Δ_1° and Δ_2° likely to be similar, and the contribution from $[Pr(DMP)_2^+]$ small in any case, it was assumed that Δ_1° and Δ_2° were equal. The observation equation is reduced to

$$\Delta_{obs} = \left\{ \frac{[ML^{2+}] + 2[ML_2^+]}{[L_T]} \right\} \Delta^\circ \qquad (13)$$

with three parameters Δ°, β_1, and β_2. The calculated parameters (and variances) are given in Table I. The results for the extended sets at 52°C (77 points) and 58°C (23 points) are clear and unambiguous. The root mean square error (σ) in Δ_{obs} is less than 0.2% of the mean value of Δ_{obs}. The larger error at 52°C arises because four sets of data are combined; systematic errors, either real differences in the activity coefficients or systematic differences of concentrations, temperatures, etc., superimpose on the random errors within a set. Note that if activity coefficients are not used, the error in Δ_{obs} is 14-fold larger (2.5 vs. 0.18 ppm). The extent of curvature in the Δ_{obs} vs. $[Pr^{3+}]$ data in the small sets at 28°C (seven points, ^1H data) and 44°C (12 points) is insufficient to give a unique fitting for three parameters. The results of fittings of β_1 and β_2 for a succession of fixed values of Δ° are given in Table I. The likely values of Δ°, β_1, and β_2 at 28 and 44°C will be discussed below.

The results of the fitting of the 52°C data are presented as a plot of the observed change in chemical shift of DMP^-, Δ_{DMP}, versus the calculated fraction of DMP^- bound in Pr^{3+} complexes (the term in braces in Eqn. 13, here called L_B/L_T or the saturation fraction) in Fig. 4. The perfect straight line extends to L_B/L_T of 0.7, where, in our conditions, $Pr(DMP)^{2+}$ is the overwhelming species. The fact that the fitting is equally good at lower L_B/L_T justifies our assumption that $\Delta_2^\circ = \Delta_1^\circ = \Delta^\circ$: below $L_B/L_T = 0.15$ the contribution from $Pr(DMP)_2^+$ slightly exceeds 20%.

The point to remember in the subsequent analysis of the DPPC results is that, from the fitting shown in Fig. 4, Δ° for the Pr^{3+}- phosphodiester complex is 91.5 ppm in water at 52°C. We have found no closely analogous data available for comparison. A tris(phosphotriester) Pr^{3+} complex exhibited downfield shifts of 83 or 76 ppm from the homologous diagmagnetic La^{3+} complex, in chloroform or n-hexane ($[Pr(OP(O-(CH_2)_4CH_3)_3)_3(NO_3)_3]$, [20]). A more tentative but more relevant value can be derived from the limiting shift calculated for a 1 : 1 Eu^{3+} phosphodiester complex in water at 30°C (L-α-glycerophosphorylcholine, a water-soluble DPPC homologue [10]). From the listed values of Δ° for the Eu^{3+}-glycerophosphorylcholine complex, the estimate of the contact contribution to this shift, and the contact and pseudocontact coefficients of Eu^{3+} and Pr^{3+}, an estimate of 118 ppm downfield for the limiting shift of ^{31}P in Pr^{3+}-

TABLE I

EQUILIBRIUM CONSTANTS AND LIMITING SHIFTS CALCULATED FOR THE [$Pr(DMP)_n^{+(3-n)}$] EQUILIBRIA AT FOUR DIFFERENT TEMPERATURES

Underlined parameter values are fixed throughout the fitting calculation.

T (°C)	$\mathring{a}$ (Å)	Δ° (σ^2) [a]	β_1 (σ^2) [a]	β_2 (σ^2) [a]	K_2 [b]	σ (Δ_{obs}) [c] (ppm)	Comments
28	6.25	4.51 (0.055)	69.74 (4.07)	414.21 (–)	5.94	0.010	^{1}H; 7 pts.
	6.20	4.00	90.1 (3.29)	722.4 (25.0)	8.02	0.009	
	6.20	4.25	79.6 (2.68)	547.88 (21.89)	6.88	0.009	
	6.20	4.75	64.3 (1.99)	338.2 (17.98)	5.26	0.009	
	6.20	5.25	53.77 (1.61)	223.5 (15.47)	4.16	0.009	
	6.20	5.75	46.13 (1.36)	154.9 (13.69)	3.36	0.009	
	6.20	6.00	43.04 (1.28)	130.8 (13.03)	3.04	0.010	
44	6.20	70	98.49 (10.5)	997.7 (33.0)	10.13	0.067	^{31}P NMR
	6.20	75	93.07 (8.62)	711.66 (13.35)	7.65	0.067	12 pts.
	6.20	80	86.0 (7.07)	513.12 (5.04)	5.97	0.067	
	6.20	85	79.11 (5.78)	374.77 (6.19)	4.74	0.068	
	6.20	90	72.58 (4.80)	276.96 (8.18)	3.82	0.068	
	6.20	95	66.76 (4.05)	206.47 (9.17)	3.09	0.068	
52	6.20	91.49 (0.39)	81.08 (0.71)	348.68 (8.56)	4.30	0.1847	^{31}P; 77 pts.
	6.10 (0.11); 6.22 (0.10)	92.86 (1.47)	80.11 (1.08)	317.66 (24.17)	3.97	0.1851	5-parameter fit
58	6.20	89.05 (3.21)	90.27 (7.68)	463.21 (78.5)	5.13	0.123	^{31}P; 23 pts.

[a] Values in parentheses represent variance, σ^2, of floating parameters.
[b] $K_2 = \beta_2/\beta_1$.
[c] The root-mean-square error, σ, in the dependent variable, Δ_{obs}.

glycerophosphorylcholine in water at 30°C can be obtained. Since both the contact and pseudocontact contributions to Δ° (68% and 32%, respectively, at 30°C [10]) are downfield, the magnitude of Δ° is expected to be inversely proportional to temperature [21].

We do not wish to place a great deal of weight on the temperature dependence of our constants, since only two points, 52 and 58°C, gave unambiguous results. However, these data do show a decrease in Δ° between 52 and 58°C as expected from the above, and suggest in turn that the β values at 44°C for the fitting with $\Delta^\circ > 90$ ppm are more likely. To the extent that the change in β_1 between 52°C and 58°C can be taken seriously, the formation of $Pr(DMP)^{2+}$ has a ΔH_1° of +3.8 kcal/mol and a ΔS_1° of +15 cal/deg per mol (cf. the result for Pr^{3+} and isobutyrate, in 2 M ionic strength, of 3.02 kcal/mol and 18.4 cal/deg per mol [22]). If ΔH_1° does not vary greatly with temperature, β_1 will have values of 51 M^{-1} at 28°C and 70 M^{-1} at 44°C. The corresponding values of Δ° are 5.5 ppm (^{1}H, 28°C) and 92.5 ppm (^{31}P, 44°C) (Table I); the latter value exhibits the expected trend with temperature. A positive enthalpy and moderately large entropy of formation are interpreted as indicative of 'inner sphere' complexation (Ref. 23 and references therein), which is consistent with a substantial contact contribution (see above) to the Pr^{3+}-induced ^{31}P hyperfine shift in DMP^-. The positive enthalpy for mono-complex formation of 3.8 kcal/mol dictates the change in Δ_{obs} with increasing temperature in most solutions, despite the fact that Δ° is decreasing: in a solution 78 mM in NaDMP and 164 mM in $Pr(NO_3)_3$, Δ_{obs} increases linearly, with a slope of 13.6 Hz/deg, between 30 and 56°C.

With regard to the magnitudes of our equilibrium constants, there again seems to be little in the literature for direct comparison. Hauser and co-workers have reported a value of K_1 ($= \beta_1$) for the binding of Pr^{3+} to a relevant phosphate ester anion, phosphoryl-

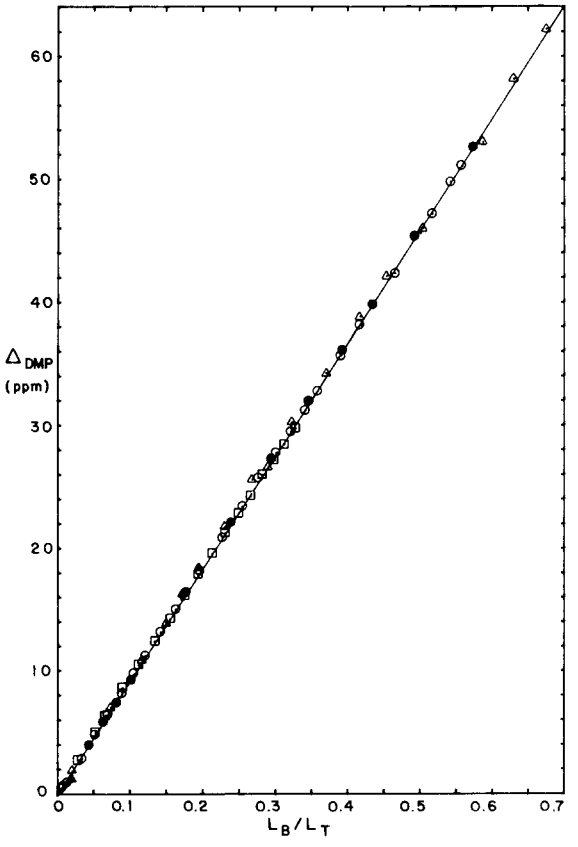

Fig. 4. Chemical shift for the DMP phosphorus resonance plotted vs. the ratio of bound DMP^- to total DMP^- (L_B/L_T) at 52°C. The 77 data points cover the same [DMP] ranges given in Fig. 3 and are represented by the same symbols. The solid line represents the calculated values from a fitting with a limiting shift for DMP bound to Pr^{3+} of 91.49 ppm (for this calculation, β_1 was 81.08, β_2 was 348.68, and δ was held at 6.20 (not iterated), see Table I).

choline, to be 5.2 M^{-1} (28°C, pH 5.7, in the presence of Ca^{2+}) [6]. Since this appears to be concentration equilibrium constant, it is actually in rather good agreement with our thermodynamic constant (the latter should be about an order of magnitude greater than the former at normal ionic strengths (see Fig. 3)). Both Hauser et al. [6] and Westman and Eriksson [10] have reported values for the binding of Eu^{3+} to glycerophosphorylcholine; giving 7.8 M^{-1} (28°C, pH 6.1, in the presence of Cd^{2+}) [6] and 2.9 M^{-1} (30°C, pH 4) [10] for the K_1 of this interaction. These both appear to be concentration equilibrium quotients. The value of K_1 ($=\beta_1$) which we find for Pr^{3+}/DMP^- (80 M^{-1} at 52°C) is clearly large enough such that we can ignore complications due to complexation by NO_3^- (the concentration constant for NO_3^- binding to Nd^{3+} at 0.6 M ionic strength, 25°C, is 1.1 M^{-1} (Ref. 24 and references therein), ΔH° is negative for Eu^{3+} binding [25]).

The binding of praseodymium(III) to the outer vesicle surface

When vesicles comprised of DPPC are present along with DMP^-, the vesicle surface competes, very successfully, with the DMP^- for Pr^{3+} ions [5]. This can be seen from a comparison of the values of Δ_{obs} for DMP^-, Δ_{DMP} (set out in Table II, along with other data), for roughly constant DMP^- and Pr^{3+} concentrations with varying DPPC concentrations *. The converse of this (i.e., competition of DMP^- with DPPC) is clearly seen in Fig. 5 which depicts the NMR titration curves of Δ_{obs} for the outer surface DPPC, $\Delta_{DPPC,o}$, with added Pr^{3+} in the presence of different concentrations of DMP^-.

As has been said, the amount of Pr^{3+} bound to DPPC on the outer vesicle surface is determined without reference to $\Delta_{DPPC,o}$: it is the known amount of added Pr^{3+} less the free Pr^{3+} and the Pr^{3+} bound to DMP^- (the latter two values determined accurately from Δ_{DMP}, as above). A priori, the stoichiometry of the surface binding is unknown, and might be variable (mono, bis, tris...). If, however, the average stoichiometry, $\bar{n}$, does not change in the Pr^{3+}/DPPC ratio interval studied (in particular if a unique stoichiometry, say $n = 1$ or $n = 2$ exclusively, obtains), the NMR observation equation takes the form of a straight line of slope $\bar{n}\Delta^\circ_{DPPC,o}$.

$$\Delta_{DPPC,o} = \frac{[Pr(DPPC)_{\bar{n}}]}{[DPPC]_o}\ \bar{n}\ \Delta^\circ_{DPPC,o} \qquad (14)$$

The concentrations of bound Pr^{3+} and the values of $\Delta_{DPPC,o}$ are both known, and their relationship is indeed reasonably linear (Fig. 6). The least-squares straight line through the data is shown and extrapolates to a value of 181.6 ppm (downfield) for $\bar{n}$.

* Whenever Pr^{3+} alone is removed from the outer solution, whether by dialysis or by resonication (such that some Pr^{3+} enters the insides of the vesicles), the value of Δ_{DMP} always decreases to a greater extent than $\Delta_{DPPC,o}$.

TABLE II

EXPERIMENTAL CONCENTRATIONS AND CHEMICAL SHIFTS FOR THE DPPC VESICLE-NaDMP-$Pr(NO_3)_3$ SYSTEM (T = 52°C)

Data set [a]	$[Pr(NO_3)_3]$ [b] (M)	[NaDMP] [c] (M)	$[DPPC]_o$ [d] (M)	Δ_{DMP} [e] (ppm)	$\Delta_{DPPC,o}$ [e] (ppm)
A	0.00206	0.0455	0.0521	0.91	5.01
	0.00409	0.0453	0.0518	2.33	7.41
	0.00810	0.0448	0.0512	5.52	11.14
	0.01201	0.0443	0.0507	8.49	14.30
	0.01589	0.0439	0.0500	11.23	17.23
	0.01966	0.0434	0.0496	13.65	19.92
B	0.00144	0.1104	0.0624	0.29	3.36
	0.00288	0.1100	0.0620	0.88	5.78
	0.00430	0.1096	0.0617	1.52	7.41
	0.00572	0.1093	0.0614	2.22	8.54
	0.00711	0.1088	0.0611	2.94	9.88
	0.00850	0.1085	0.0608	3.62	11.06
	0.00988	0.1081	0.0603	4.34	12.00
	0.01124	0.1078	0.0600	4.75	13.18
C	0.00405	0.0974	0.0491	2.05	6.91
	0.00799	0.0961	0.0484	3.80	9.88
	0.01184	0.0949	0.0478	5.95	12.72
D	0.00370	0.0931	0.0408	1.48	6.59
	0.00722	0.0922	0.0404	3.65	10.17
	0.01073	0.0913	0.0401	5.82	12.94
	0.01394	0.0904	0.0396	7.77	15.55
	0.01754	0.0896	0.0393	9.60	17.85
	0.02084	0.0888	0.0389	11.46	20.34
	0.02410	0.0879	0.0385	13.40	22.79
E	0.00288	0.1851	0.0420	1.00	4.39
	0.00577	0.1851	0.0420	2.02	7.16
	0.00853	0.1839	0.0413	3.11	9.43

[a] For reference to Figs. 5–11: A (○); B (△); C (▲); D (□); E (●).

[b] Concentration is corrected for presence in the extravesicular space.

[c] Concentration is corrected to exclude that volume occupied by DPPC.

[d] Concentration is outer surface DPPC/extravesicular volume.

[e] The values of Δ_{DMP} and $\Delta_{DPPC,o}$ are approximated in this work by the splittings between the outer and inner resonances (see Fig. 1). Although this is not strictly correct, the inner resonances do suffer a small hyperfine shift [26]; the errors for our studies are never more than 5% and usually much less.

$\Delta^{\circ}_{DPPC,o}$. This, of course, would be the value of $\Delta^{\circ}_{DPPC,o}$ if there were exclusive 1 : 1 stoichiometry (i.e., $Pr(DPPC)^{3+}$, $n = 1$). If there were exclusive 1 : 2 stoichiometry (i.e., $Pr(DPPC)_2^{3+}$), then $n = 2$ and $\Delta^{\circ}_{DPPC,o}$ would equal 90.8 ppm. It is interesting to recall the value we determine for the DMP^- limiting shift, Δ°_{DMP}, at this temperature, 91.49 ppm. For reasons discussed in detail below, it is out of the question that the two Δ° values should differ by a factor of 2; in fact they should be similar *. The necessary conclusion is that $n = 2$, i.e., that essentially exclusive 1 : 2 stoichiometry obtains on the outer phosphatidyl-

* The mode of binding of Pr^{3+} to the two phosphodiesters, DMP^- and DPPC, should be the same. This certainly entails binding through the same ligative atom; surely non-esterified oxygen in each case. Whether it also entails the same degree of 'denticity' is not clear. The DMP^- is most likely a bidentate ligand in this case.

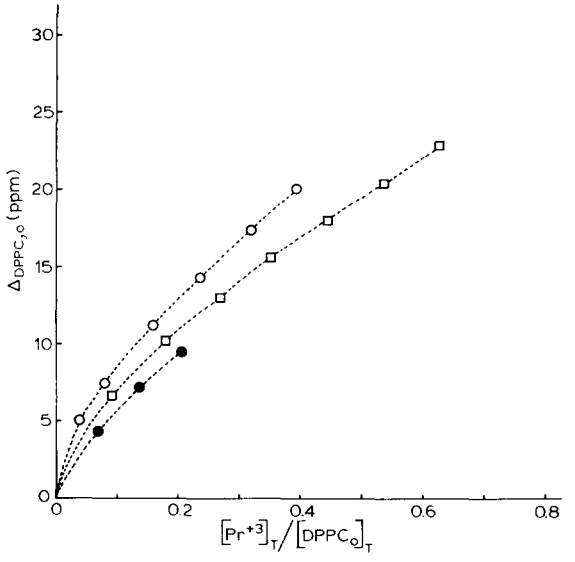

Fig. 5. The observed downfield shift of the outer DPPC resonance with increasing Pr^{3+} concentration, at different DMP^- concentrations. Notice that the DPPC concentrations are roughly the same (○, 52.1 mM to 49.6 mM; □, 40.8 mM to 38.5 mM; and ●, 42.0 mM to 41.3 mM) and that the DMP^- concentrations are roughly constant for each curve (○, 45.5 mM to 43.4 mM; □, 93.1 mM to 87.9 mM; and ●, 185.1 mM to 183.9 mM). These plots represent data sets A, D and E of Table II. The dashed curves are not fittings but are intended solely to guide the eye. The temperature is 52°C.

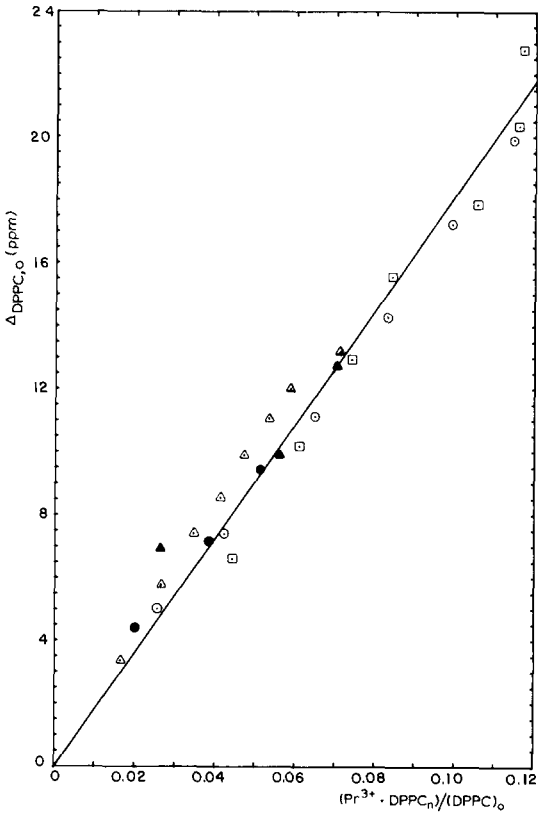

Fig. 6. Chemical shift for the ^{31}P-NMR peak of outer DPPC as a function of the ratio of DPPC-bound Pr^{3+} to total outer DPPC at 52°C. The solid line represents the calculated values with a limiting shift of 181.6 ppm for $n = 1$ for Pr^{3+} DPPC binding. (Refer to Table II for correlation of experimental points to symbols.)

choline bilayer surface. The result reported here is in fact the first solid evidence for such a conclusion.

The derived concentrations of DPPC-bound Pr^{3+} and free Pr^{3+} are plotted in Fig. 7. Evaluation of the binding equilibria is not as straightforward as the limiting shift. In an attempt to maintain both clarity and simplicity in the equilibrium equations to be discussed, we will represent the concentrations of species with the following symbols, in a manner analogous to that for the Pr^{3+}/DMP^- system: $[MP_n]$ is the concentration of Pr^{3+} bound to the outer DPPC surface, [M] is the concentration of free Pr^{3+}, $[M]_T$ the total outer concentration of Pr^{3+}, [P] the concentration of free outer DPPC, and $[P]_T$ the total concentration of DPPC *.

The simplest surface absorption model, the Langmuir isotherm (or Volmer isotherm [27]), assumes no interactions between distinct, discrete surface binding sites, whether occupied or not. It is expressed in Eqn. 15, where θ represents the fraction of

$$K_L = \frac{\theta}{(1-\theta)[M]} \qquad (15)$$

surface sites filled. Using the symbols defined above,

* 'Concentration', as used here, simply represents the number of moles of a species, even if it is constrained to the outer vesicle surface, divided by the number of dm^3 of outer aqueous volume. See footnotes to Table II. When a surface concentration is really required, such as for charge density in Eqn. 16, it is implicitly incorporated.

$\theta = n[MP_n]/[P]_T$. The result of fitting Eqn. 15 to our data with K_L and n as adjustable parameters (n was allowed only integral values) is also shown in Fig. 7. The best fitting was obtained for $K_L = 435$ and $n = 7$. The latter value seems obviously unreasonable on its own merits and is clearly in disagreement with our conclusion, based on the value of $\Delta^{\circ}_{DPPC,O}$, that $n = 2$. Since the bound ions are expected to interact with each other, at least electrostatically, the Langmuir isotherm is not really expected to give a good description of the binding and thus was not considered further.

The equation most frequently used to express the effects of electrostatic interactions on the binding of charged species to macroscopic membrane surfaces is the Stern equation [27]; a Debye-Hückel-like solution for an infinite plane with uniform smeared surface-charge density σ (charge/area). The binding isotherm is given in Eqn. 16 where the amount of

$$K_s = \frac{\sigma}{(\sigma_{max} - \sigma)\{[M]_\infty \exp(-ze\psi_o/kT)\}} \quad (16)$$

bound Pr^{3+} is related to the charge density, σ, produced by the binding; σ_{max} is given by $ze/(A_h n)$ (where z is the signed charge of Pr^{3+}, e is the unsigned magnitude of the electronic charge, and A_h is the area per headgroup), $[M]_\infty$ is the concentration of free Pr^{3+} in the bulk (i.e., at a relatively great distance from the membrane surface), and ψ_0 is the surface electrical potential (relative to the potential of the bulk aqueous phase). However, the magnitude of ψ_0 is itself a function of σ and the relationship, in a mixed electrolyte solution, is given by the Grahame equation (17) (based on the Gouy equation), where, ϵ_0 is the permittivity of

$$\sigma = \left\{ 2\epsilon_o \epsilon_r \frac{kTN}{10^3} \times \sum_i C_{i,\infty}[\exp(-z_i e\psi_0/kT) - 1] \right\}^{1/2} \quad (17)$$

free space, ϵ_r is the dieletric constant, the summation is taken over all ions, i, in the solution, $C_{i,\infty}$ is the concentration of the ith electrolyte in the bulk aqueous phase, and the z_i is the signed charge of the ith species [29]. The combination of Eqns. 16 and 17 to eliminate ψ_0 is called a Stern isotherm and has proved to provide good descriptions of a number of ion membrane binding equilibria ([27], notice that our K_s is a binding constant, whereas McLaughlin's K_s is a dissociation constant; likewise for K_L).

We have compared the predictions of Stern isotherms with our data and the results are shown in Fig. 8. Theoretical curves for the cases where $K_s = 10^5$, 10^4 and 10^3, each with [NaDMP] equal to either 0.05 M or 0.10 M, are shown. In calculating each of these curves, a value of $\sigma_{max} = 95\,298$ e.s.u./cm^2 ($n = 2$, $A_h = 75$ Å^2 [15]) was used. The predictions of the Stern equation do not fit our data on two separate counts: first, the observed binding isotherm has the wrong shape, increasing much more steeply with $[Pr^{3+}]$ than predicted *; second, the observed isotherms for various NaDMP concentrations (0.043 to 0.185 M, Table II) show almost no differences, whereas the Stern isotherm predicts a strong ionic-strength dependence.

Since the real isotherm shows smaller effects of electrostatic repulsion than predicted, some form of effective 'cooperativity' on binding of Pr^{3+} is indicated. For orientation purposes, the Hill equation was therefore fitted to the data. The Hill equation is given as (18) (Ref. 30; K_{app} is defined

$$K_H = \frac{n[MP_n]}{[P][M]^c} = \frac{K_{app}}{[M]^{c-1}} \quad (18)$$

in Eqn. 19), where c is an empirical constant. In the Hill plot, i.e., $\log\{n[MP_n]/[P]\}$ vs. $\log[M]$, the slope is c and the intercept $\log K_H$. Such a plot of our data, with $n = 2$, is shown in Fig. 9. The linear correlation is observed to be quite good and a linear least-squares analysis yields a value of K_H equal to 4.25 and c equal to 0.543 with a root-mean-square error, in $n[MP_n]/[P]$, of 0.009. A value of c less than 1 indicates a negative cooperativity in the binding. However, one would expect the electrostatic repulsion discussed above to be manifest as a negative cooperativity. Indeed, if one makes a Hill plot of the theoretical Stern curve representing $K_s = 10^4$ and [NaDMP] =

* The only way to force the theoretical curves into a good fitting would be to increase σ_{max} to values considerably greater than that representing one Pr^{3+} bound per DPPC molecule. This would correspond to $n \ll 1$.

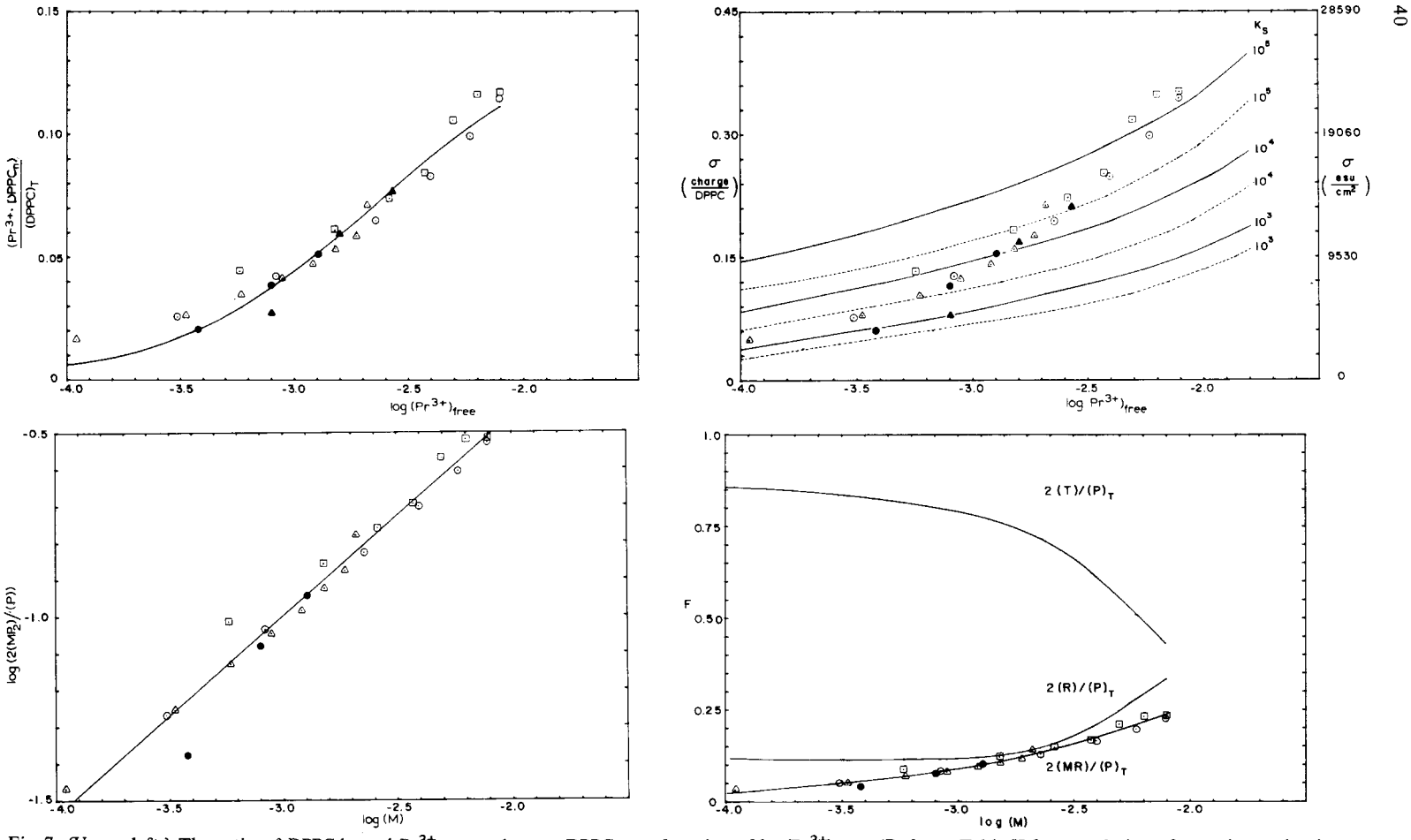

Fig. 7. (Upper left.) The ratio of DPPC-bound Pr^{3+} to total outer DPPC as a function of $\log(Pr^{3+})_{free}$. (Refer to Table II for correlation of experimental points to symbols). The smooth curve represents a Langmuir binding isotherm calculated on the basis of $n = 7$ and $K_L = 435$.

Fig. 8. (Upper right.) Several Stern binding isotherms calculated on the basis of $n = 2$, $A_h = 75$ Å^2, and thus $\sigma_{max} = 95\,298$ e.s.u./cm^2 (- - - - -, [NaDMP] = 0.05 M; ———, [NaDMP] = 0.10 M; refer to Table II for correlation of experimental points to symbols).

Fig. 9. (Lower left.) The best calculated fit for $[Pr(DPPC)_2]^{3+}$ binding based on the Hill equation (refer to Eqn. 18) with $K_H = 4.25$ and $c = 0.543$. (Refer to Table II for correlation of experimental points to symbols.)

Fig. 10. (Lower right.) The fraction, F, of outer DPPC to the total outer DPPC in a given state as calculated on the basis of the two-state model. ($K_C^\circ = 0.136$, $K_T^\circ = 2.02$, $K_R^\circ = 1\,500 \cdot K_T^\circ$, $f = 0.005$; refer to Table II for correlation of experimental points to symbols.)

0.10 M in Fig. 8, one obtains a straight line with a slope of $c = 0.26$ *. Thus, although our data indicate an overall negative cooperativity, they indicate a positive cooperativity relative to the Stern theory. A source for this relative positive cooperativity must be sought.

Ad hoc equations incorporating both electrostatic repulsion and a higher-order attraction can fit the data moderately well, with parameters that indicate a highly-screened electrostatic environment **. However, we also desired a model which would fit the data while giving some insight into the finer details of the binding process.

There are a number of pieces of independent evidence in the literature that the binding of Ln^{3+} ions to the surface of phosphatidylcholine bilayers induces a lipid conformational change in the headgroup region [10,31–34]. Such a change would seem quite likely to have an effect on the ion binding property of the surface. Thus, we have considered a two-state model structured in the following manner. The state of the surface in the absence of bound ions, which we shall refer to as the T state, is one where the headgroup conformation is such as to provide a relatively low affinity for Pr^{3+}. As Pr^{3+} binds to the surface, a conformational change requiring some intrinsic gain of free energy occurs, but results in a net loss in free energy because the affinity for Pr^{3+} in the new conformational state, R, is much higher than that in T. We formulate this model in terms of the following equilibria; where K_c^o, K_T^o, K_R^o, k, a and f are adjustable parameters. Notice that, for the two metal binding equilibria, we

$$T \rightleftharpoons R\ ; \qquad K_c = \frac{[R]}{[T]} = K_c^o(1 + kZ^a) \tag{23}$$

$$M + T \rightleftharpoons MT\ ; \qquad K_T = \frac{[MT]}{[M][T]} = K_T^o \exp(-fZ) \tag{24}$$

$$M + R \rightleftharpoons MR\ ; \qquad K_R = \frac{[MR]}{[M][R]} = K_R^o \exp(-fZ) \tag{25}$$

have retained the simple electrostatic term exponential in total vesicular charge, Z (Eqn. 21). The apparent equilibrium constant, K_{app}, is then represented as in Eqn. 26, where $q = K_R/K_T = K_R^o/K_T^o$.

$$K_{app} = \frac{[MR] + [MT]}{[M]([R] + [T])} = \frac{K_T^o \exp(-fZ)(1 + K_c q)}{(1 + K_c)} \tag{26}$$

In fitting this model to our data, we generally allowed only K_T^o and K_c^o to float, holding the other parameters fixed throughout a given fitting. With this approach to the fittings, the better values of q are found to be in the range 1 000 to 2 000, the best value of a is 4, f ranges from $4.5 \cdot 10^{-3}$ to $5 \cdot 10^{-3}$ (see earlier footnote) and k from $4/(750)^4$ to $6/(750)^4$. A listing of the parameters and errors for the better fittings is given in Table III and a graphical depiction of one of these is presented in Fig. 10 which shows the fraction of DPPC in a given state as a function of

---

* The value of c is even smaller for the Stern curve with $K_s = 10^4$ and [NaDMP] = 0.05 M and would probably increase only slightly for the $K_s = 10^5$ curves. The value of c is equal to 1 for a Langmuir curve.

** The data shown in Fig. 7 can be quite nicely fitted by more empirical expressions, such as

$$K_{app} = \frac{n[MP_n]}{[M][P]} = K_0 \exp(-fZ) \tag{19}$$

(best fitting: $K_0 = 198.5$, $f = 24 \cdot 10^{-4}$, see Fig. 11) or

$$K_{app} = K_0 \exp(-f_1 Z + f_2 Z^2) \tag{20}$$

(best fitting: $K_0 = 273.4$, $f_1 = 40 \cdot 10^{-4}$, $f_2 = 53 \cdot 10^{-4}$, see Fig. 11) where K_0 and f (or f_1 and f_2) are adjustable parameters and Z is the total charge on an average vesicle (Eqn. 21),

$$Z = 2000 \times 3 \times \left\{ \frac{[MP_n]}{[P]_T} \right\} = \frac{6000\,\theta}{n} \tag{21}$$

assuming 2 000 outer phospholipid molecules per vesicle [15]. It is possible to interpret f in terms of the electrostatic contribution to the binding free energy, ΔG_{el}^0,

$$f = \frac{\Delta G_{el}^0}{ZRT} = \frac{2 \times 3 \times N \times W_{el}}{Z^2 RT} \tag{22}$$

or the work required to charge up the vesicle, W_{el} [28]. We have done this, and we find that the best value of f, given above, is consistent only with a very high local ionic strength (at least 10 M) at the surface of a non-hydrated vesicle or zero distance of closest approach, δ, for counter anions to such a vesicle. A model of a vesicle hydrated in the surface headgroup annulus can reproduce the value of f given above at more reasonable local ionic strengths, if approx. 50% of the annular volume is hydrated.

TABLE III

EQUILIBRIUM CONSTANTS AND OTHER PARAMETERS CALCULATED FOR VARIOUS FITS OF THE TWO-STATE MODEL FOR Pr^{3+} BINDING TO OUTER SURFACE DPPC

K_R° [a]	k [a]	f [a]	K_C° (σ^2)	K_T° (σ^2)	σ [b]
$10^3\ K_T^\circ$	5/750[4]	0.0040	0.416 (0.105)	0.954 (0.132)	0.0095
		0.0045	0.220 (0.060)	1.785 (0.330)	0.0093
	6/750[4]	0.0050	0.135 (0.040)	3.034 (0.673)	0.0093
$1\,500\ K_T^\circ$	4/750[4]	0.0045	0.170 (0.057)	1.523 (0.375)	0.0094
		0.0050	0.062 (0.039)	4.40 (2.37)	0.0097
	6/750[4]	0.0050	0.136 (0.040)	2.02 (0.44)	0.0093
$2\,000\ K_T^\circ$	6/750[4]	0.0050	0.136	1.51	0.0093

[a] Parameters were fixed throughout a given fitting.
[b] Root mean square error in the variable, $2\ ([MR] + [MT])/[P]_T$.

$\log[Pr^{3+}]_{free}$. It is clear that, according to this model, Pr^{3+} binds essentially only to R state sites and the fraction of free R state sites increases with increasing Pr^{3+} binding. The best values of K_T° correspond closely to the best value of K_H found from the Hill analysis and, it will be noted, are significantly less than the value of β_2 for the DMP^- binding at 52°C (Table I) while the K_R° values are, of course, significantly greater.

A comparison among the best fittings for the various models is presented in Fig. 11 in terms of the relative error in the dependent variable, the fraction of bound sites to total sites, $\theta = n[MP_n]/[P]_T$. The relative error is defined as the ratio of the observed value to the calculated value of the dependent variable. The results of the two-site fitting are slightly better than the empirical fittings (Eqns. 19 and 20), and are more satisfying in terms of a physical picture.

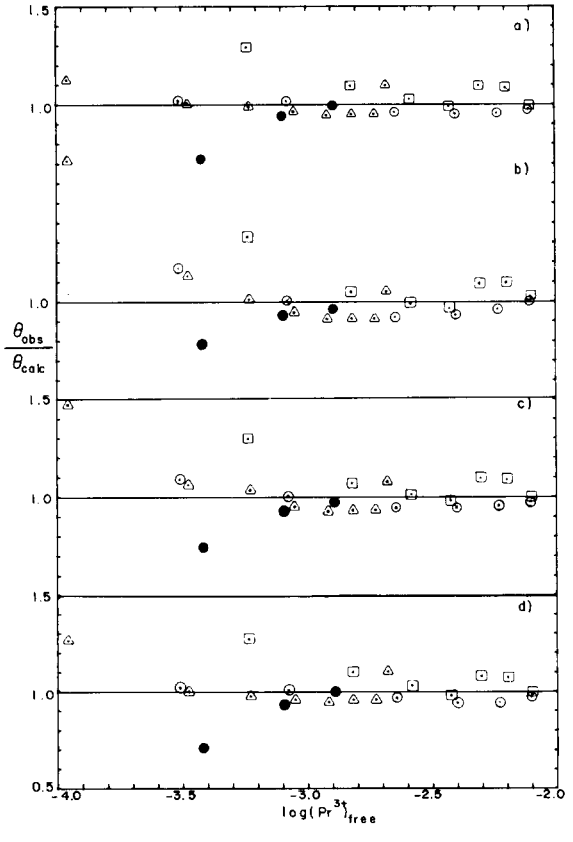

Fig. 11. Relative error plots for $\theta_{obs}/\theta_{calc}$, the ratio of observed Pr^{3+} bound DPPC over the total DPPC (θ_{obs}) to the calculated value. a. Hill equation (Eqn. 18). b. Empirical electrostatic equation with a single electrostatic term (refer to Eqn. 19). c. Empirical electrostatic equation with two electrostatic terms (refer to Eqn. 20). d. Two-state model (refer to Fig. 10). (Refer to Table II for correlation of experimental points to symbols).

Inner surface vs. outer surface binding

All of the above work has dealt with Pr^{3+} binding to the outer vesicle surface. Although an inner surface Pr^{3+} binding (^1H) NMR isotherm has been presented [35], no analysis has been made. In previous reports [2,5], we have indicated that binding to the inner vesicle surface apparently differs from outer surface binding in geometry and/or intrinsic binding capacity.

TABLE IV

Pr^{3+} BINDING TO VESICULAR INNER SURFACES (DATA OBTAINED AT 52°C)

$[Pr^{3+}]_{free}$ (mM)	$[Pr(DPPC)]_i/[DPPC]_{i,T}$	$[Pr(DPPC)]_o/[DPPC]_{o,T}$	$n\Delta^{\circ}_{DPPC,i}$ (ppm)
2.05	0.1947	0.0693	81.7
1.41	0.1414	0.0525	84.1

A couple of preliminary experiments to characterize this difference have been conducted.

In these experiments, vesicles were prepared by ultrasonic irradiation in the presence of $Pr(NO_3)_3$ as well as NaDMP. Thus, the final vesicles contain Pr^{3+} (and DMP^-) in the inner aqueous phase. Assuming the free Pr^{3+} concentration is the same in both aqueous regions, the observed Δ_{DMP} value, as before, allows us to determine the amount of Pr^{3+} bound to DPPC, on both outer and inner surfaces. Now, the fraction of Pr^{3+}-bound DPPC on the outside surfaces can be determined from our knowledge of the limiting shift for the outer surface, via Eqn. 14 ($\bar{n} = 2$), and the observed value of $\Delta_{DPPC,o}$, which is always found to be less than $\Delta_{DPPC,i}$. (In these experiments, $\Delta_{DPPC,i}/\Delta_{DPPC,o} = 1.26$; even for different ratios of $[Pr^{3+}]_T$ to $[DPPC]_T$.) Thus, the amount of Pr^{3+} bound to the inner surface at the same free Pr^{3+} concentration is simply the difference between the total Pr^{3+} and the sum of DMP-bound Pr^{3+} and outer DPPC-bound Pr^{3+}. Since this is determined without recourse to the observed value of $\Delta_{DPPC,i}$, this quantity is available for an independent estimation of $\Delta^{\circ}_{DPPC,i}$ (assuming an exclusive binding stoichiometry).

For our two preliminary experiments, we find the results listed in Table IV. We see that the inner binding is approx. 3-times greater than the outer binding. Also, the values of $n\Delta^{\circ}_{DPPC,i}$ would be quite consistent with our more extensive determinations of Δ°_{DMP} and $\Delta^{\circ}_{DPPC,o}$ above if $n = 1$ for the inner surface. Thus, it would seem that the inner surface presents binding sites for polyvalent metal cations in yet a third headgroup conformational state.

Discussion

There has been considerable discussion of the stoichiometry of Ln^{3+} binding to phosphatidylcholine bilayers (Refs. 5 and 10 and references cited therein). Our data represent the strongest evidence to date that, at least for DPPC, an Ln^{3+} ion binds directly to two lipid molecules on the outer vesicular surface when the bilayer is in the fluid state. The argument with which Hauser et al. [6] also reached this conclusion is internally inconsistent and fundamentally flawed: they used the equation

$$K_{obs} = K_0 \exp -a\frac{[ML_n]}{[L_T]} = \frac{[ML_n]}{[M^{3+}][L_T - n\,ML_n]^n} \quad (27)$$

which is inappropriate for binding to sites like the phospholipid vesicle surface. Binding to quasi-solid surface sites, even if the ligands can diffuse (as they do in solids also), does not incur the entropy loss associated with binding of dilute ligands that had been freely translating in three dimensions [9]. The $[L_T - nML_n]$ factor in Eqn. 27 must have the exponent $n = 1$. Morever, their fits to $n = 1$ and $n = 2$ (see their Fig. 6) are not distinguishable in quality, and both suffer the contradiction that log K_{obs} is not, as they would predict from Eqn. 27, linear in $[ML_n]/[L_T]$. It is not clear why the value of $[ML_n]/[L_T]$ for which log K_{obs} is zero should be a unique point, but in any case, a proper log K_{obs} in which n does not figure as an exponent, gives plots for $n = 1$ or $n = 2$ which are very close together (not separated by what amounts to log $[L_T]$), and their argument favoring $n = 2$ falls to the ground.

Our conclusion on the stoichiometry is based on the comparison of the DMP^- and DPPC limiting Pr^{3+} hyperfine shifts, i.e., the near equality of the ratios Δ°_{DMP}/n and $\Delta^{\circ}_{DPPC,o}/n$ (91 ppm downfield, at 52°C). As mentioned above, our value is in good agreement

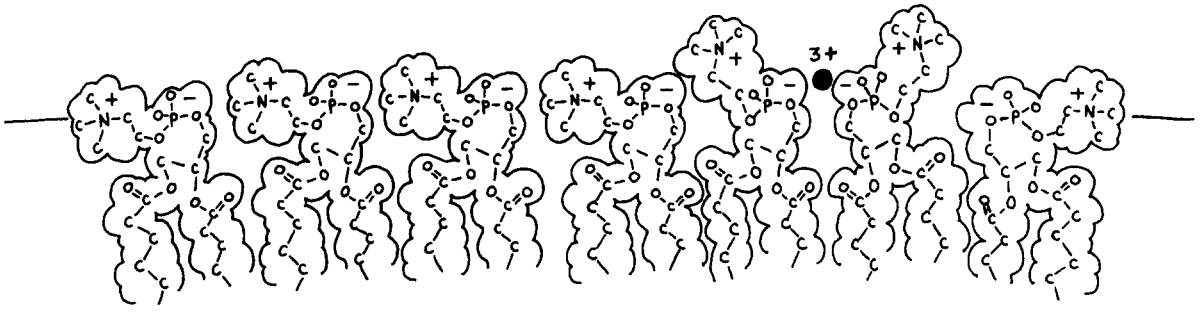

Fig. 12. Molecular diagram depicting the proposed headgroup conformational change upon polyvalent metal ion binding to the surface of a phosphatidylcholine bilayer membrane. Detailed precision in bond lengths and bond angles is not meant to be implied. The figure is derived from one by Yeagle [36].

with one we would calculate for the 1 : 1 complex of Pr^{3+} with glycerophosphorylcholine using the hyperfine coefficients of Westman and Eriksson [10]. This makes it puzzling as to why Westman and Eriksson are not concerned that, for Eu^{3+} at 30°C, they find that the products are equal, $n\Delta^{\circ}_{GPC} = n\Delta^{\circ}_{EL,o}$, (rather than the ratios) when $n = 1$ for glycerophosphorylcholine (GPC) and $n = 2$ for egg lecithin (EL) *. It seems quite likely that their value for $\Delta^{\circ}_{EL,o}$ is in error. This value depends on the fitting of the surface binding data to an isotherm which has the same fundamental problem as that of Hauser et al. In addition, this error, pointed out by McLaughlin et al. [9], makes it impossible to compare the magnitudes of our surface binding constants with those of Hauser et al. or of Westman and Eriksson; the most complete studies of Ln^{3+} binding to phospholipid bilayer surfaces to date.

The most interesting aspect of our data is that they correspond to binding not as anticooperative as that predicted by Stern theory. A diagram depicting a headgroup conformational change which could be involved in our suggested cooperative model is shown in Fig. 12. The figure is derived from one published by Yeagle [36] and is not meant to imply detailed precision in bond lengths or angles. Indeed, the dynamic membrane surface structure is certainly not yet known with overwhelming precision [37]. The region of the bilayer surface in the left of the figure suggests a more folded headgroup conformation, with zwitterionic dipoles lying roughly parallel to the surface, agreed by most to be the state of the phosphatidylcholine surface in the absence of metal cation binding [36,38]. This can be thought to represent the T state of the DPPC bilayer in the fluid phase. Although it was once thought that the binding of Ln^{3+} ions produced no change of headgroup conformation [39], there has been mounting independent evidence that such a change occurs [10,31–34], and that it involves a bending of the headgroup away from the surface [31]. One might expect the Ln^{3+} bound to the phosphate moiety to repel the quaternary $-N(CH_3)_3^+$ group. Such a structure, depicted on the right in Fig. 12, could be thought to represent the R state of the DPPC surface. Structures similar to the two shown in Fig. 12 have been found by X-ray diffraction analysis [40]. An increasing amount of bound Ln^{3+} in R-state sites could have an allosteric effect producing even more high-affinity R-state sites on the membrane surface. Sears, Hutton and Thompson postulated the existence of high and low affinity Ln^{3+} binding sites on the surface of phosphatidylcholine vesicles [41], but their proposal differs from ours in that they considered the proportions of the sites to be fixed and the Ln^{3+} exchange between sites to be slow on the NMR scale. A remarkably prescient depiction of such a headgroup conformational change was published by Michaelson, Horwitz and Klein several years ago [42]. It is also quite possible that our model is reflecting a phase change (with concomitant lateral phase separation) triggered by Ln^{3+} binding. There is some evidence that such binding would be stronger in the gel phase [26,43]. This subject, and the possible cooperative consequences, is beginning to

* Thus, were we to calculate $\Delta^{\circ}_{EL,o}$ for Pr^{3+} at 30°C, using their value for Eu^{3+} and their hyperfine coefficients, we would obtain a value of 52 ppm, downfield.

attract theoretical interest [44].

We have noted above that the extent of binding of Pr^{3+} to the DPPC vesicle surface does not show any significant dependence on the ionic strength of the aqueous phase, dominated, in our case, by the NaDMP salt. We offer the following observations. The headgroup annulus contains a much higher concentration of positively and negatively charged groups than the bulk solution (4.6 M, if the phosphate and $-N(CH_3)_3^+$ groups are distributed in an annulus with radii of 105 and 110 Å). Perhaps the binding of Pr^{3+} results in a redistribution of charge and/or a change in the annular dimensions (and so of local ionic strength) that is a far more effective shield than the counterion atmosphere of bulk solution ions. If the cooperativity among R sites is a manifestation of lateral phase separation, the region of high cationic charge might also provoke 'territorial' binding of freely-translating counter-anions, which is also relatively independent of ionic strength [7]. These two effects need not be separate phenomena.

We have pointed out elsewhere that, in addition to Debye shielding, the addition of salt can have at least three other effects on Ln^{3+} lipid bilayer binding (Grandjean, J., unpublished data). The binding can be decreased by sequestration of the Ln^{3+} by the added anion. The binding can be decreased by competition for the Ln^{3+} binding sites by the added cation. The binding can be increased by anion condensation (or co-condensation, along with Ln^{3+}) on the membrane surface. The first effect clearly dominates for the addition of NaDMP. The Na^+ cations do not compete significantly with Ln^{3+} for the surface (Grandjean, J., unpublished data). Additional evidence that DMP^- does not significantly bind to the DPPC bilayer, at least in the absence of Pr^{3+}, has been inferred from DMP^- ^{31}P longitudinal relaxation time, T_1, data [15]. Hauser et al. [6] and Westman and Eriksson [10] both postulated weak Cl^- binding to the egg lecithin vesicle bilayer to help in fitting their Ln^{3+} binding isotherms. The cooperativity which we postulate here could be used to give the same effect; i.e., somewhat increased Ln^{3+} binding.

McLaughlin and coworkers have published studies of binding of divalent metal cations to phosphatidylcholine bilayers which they have analyzed in terms of Stern isotherms [9]. Their data reach levels of bound phospholipid only about one-fifth the maximum observed in this work, while Fig. 8 shows that it is the data at the higher levels that are needed to demonstrate a departure from Stern behavior. Moreover, their best fittings required a mixed stoichiometry (sites with $n = 2$, having a 3-fold higher affinity for Co^{2+}, binding 1.5-times as much Co^{2+} as $n = 1$ sites). The latter effect might be the result of requiring adherence to the Stern equation; alternatively, the data might conform to our model except that Co^{2+}, or other divalent metal cations do not have affinities for the R site as great as that of Ln^{3+} and thus do not trigger the conformational change to the same extent. Our data do not really tell us anything about the stoichiometry of the T state because it is never significantly populated by Ln^{3+} ions (see Fig. 10). There is (weak) evidence that divalent cations cause changes in differential scanning calorimetry curves which could be attributed to headgroup conformational changes [34]. It is clear that Mg^{2+} and Ca^{2+} and, to a lesser extent, Ba^{2+} can compete with Ln^{3+} for binding to a phosphatidylcholine bilayer membrane (Ref. 6 and Grandjean, J., unpublished data). If it occurs at all, monovalent cation binding to lecithin surfaces is exceedingly weak (Grandjean, J., unpublished data and Ref. 9). Thus our model could accommodate monovalent, divalent and trivalent metal cation binding, with only the latter being strong enough to show a dominant effect on the binding due to the R state. However, the model is sufficiently complicated that its success here by no means proves its correctness. A similar view of a common mode of binding for all metal cations has recently been suggested [65].

In contrast to the Pr^{3+}/DMP^- binding, the Pr^{3+}/DPPC binding seems to be exothermic. The Δ_{obs} for the outer DPPC ^{31}P resonance becomes smaller with increasing temperature. (In a solution which is 75 mM in DPPC, 18 mM in Pr^{3+} and 45 mM in DMP^-, Δ_{obs} decreases by 1.2 Hz/deg over the range 46 to 58°C). This itself is in contrast to the outer $-N(CH_3)_3$ ^1H resonance, which experiences a greater hyperfine shift with increasing temperature, at least for egg lecithin vesicles [45]. This latter effect was attributed to a change in headgroup conformation toward a less extended structure with increasing temperature and the greater sensitivity of the mostly pseudocontact $-N(CH_3)_3$ ^1H hyperfine shift (possibly also intermolecular in nature) to structural changes.

The question of cation binding to the inner surface

may now be addressed. We have previously pointed out the different effects of the high curvature of small vesicles on phospholipid molecular structure in the inner and outer monolayers [15]. Our preliminary results here indicate that there can also be a difference in metal cation binding even when the free metal ion concentrations in the aqueous phases are the same. We have noted that under these conditions the Δ_{obs} for the inner DPPC ^{31}P resonance is always slightly greater than that for outer DPPC [2,5], although this effect is apparently too small to be observed at lower magnetic field strengths [42,45]. The results in Table IV suggest that this is due to a greater affinity of the inner surface binding sites rather than a greater value of $\Delta°$. The $-N(CH_3)_3$ ^1H resonance of the inner lecithin always exhibits a smaller value of Δ_{obs} [45,46] which must be attributed to a smaller value of $\Delta°$ than for the outer $-N(CH_3)_3$ ^1H resonance. Others have speculated that the inner headgroups have a more extended conformation due to their tighter packing relative to the outer surface [45,47] and the $\Delta°$ for the $-N(CH_3)_3$ ^1H resonance, being more sensitive to structural differences, reflects this. The apparent difference which we find for the inner site stoichiometry ($n = 1$) for Pr^{3+} binding may also be a reflection of this. We find that the $^{31}P\{^1H\}$ nuclear Overhauser effect, in the absence of metal ion binding, is very similar for the inner (approx. 30%) and outer (approx. 24%) resonances. This nuclear Overhauser effect has been found to be somewhat sensitive to headgroup conformation [36].

Our preliminary data show a substantial difference in positive charge density on the inner and outer vesicular surfaces (cf. Table IV). For example, at 2.05 mM Pr^{3+}, 201 Pr^{3+} ions are bound to the inner surface, while 136 Pr^{3+} ions are bound to the outer surface, which has more than twice the area (cf. Ref. 15 for dimensions). One can try to evaluate the potential across the hydrocarbon portion of the vesicle bilayer produced by this charge distribution and ask whether the potential would have a significant effect on transbilayer cation binding. As has been seen, straightforward Debye-Hückel theory does not adequately represent the electrostatic contribution to cation-binding behavior; it should, however, provide an upper limit to the potentials. The linearized Poisson-Boltzmann equations for an annular particle like a vesicle can be and have been solved by the method indicated in Tanford [28]. (The regions considered, starting from the center, are as follows: ion-containing solvent; the inner $-N(CH_3)_3$ surface, radius 65 Å; high dielectric constant annulus; inner phosphate + Pr^{3+} surface, radius 70 Å; low-dielectric constant annulus; outer phosphate + Pr^{3+} surface, radius 105 Å; high-D annulus; outer $-N(CH_3)_3$ surface, 110 Å; bulk solution.) At 0.11 M ionic strength, the Debye-Hückel potentials at 65, 70, 105 and 110 Å are about 250, 350, 120 and 80 mV, respectively; these are certainly overestimates. The potentials at 105 and 110 Å are not greatly decreased if the inner Pr^{3+} binding is set at zero, so that, electrostatically, cations binding to the inner and outer surfaces are nearly independent. Since, however, the total binding behavior of inner and outer surfaces is quite different (and needs a more extensive investigation), it is quite possible that differences in concentrations of strongly-binding polyvalent cations on opposite sides of a bilayer can induce curvature in a previously flat surface, even for neutral phospholipids. Lin and Macey have reported complicated cation-induced curvature changes in erythrocyte ghost membranes [48].

Other effects of curvature, for example, on the gel to liquid crystalline phase transition, have been reported [49,50,56]. These include the fact that the inner monolayer has a different thermal behavior in the phase transition region than the outer monolayer. The hydrocarbon chain regions generally require higher temperatures for melting in the outer monolayer [51], while the opposite is true of the headgroup regions [52,53]. The inner monolayer chains have a smaller theoretical order parameter than the outer monolayer chains [54,55]. Curvature effects have been found in lipid transverse distribution [57], in membrane fusion [64], and predicted for the adsorption of nonpolar molecules [58]. Membrane protein incorporation and distribution has been predicted theoretically [59] and found experimentally [60,61] to depend on curvature. The activity of phospholipase A [62] as well as that of phosphatidylcholine exchange protein [63] has been found to depend on bilayer curvature.

Acknowledgements

The authors would like to thank Drs. Hiroshi Okazaki and Fausto Ramirez for an initial gift of sodium dimethylphosphate and the reference on its

synthesis, and Drs. Alan McLaughlin, Stuart McLaughlin, Moises Eisenberg, Arthur Lau, Harold Friedman, C.V. Krishnan and Sanford Simon for stimulating discussions. We would also like to thank the National Science Foundation for support of this work (Grants PCM-76-00193 and PCM-78-07918).

References

1 Horrocks, W.DeW., Jr., Schmidt, G.F., Sudnick, D.R., Kittrell, C. and Bernheim, R. (1977) J. Am. Chem. Soc. 99, 2 378–2 380
2 Ting, D.Z., Hagan, P.S., Chan, S.I., Doll, J.D. and Springer, C.S. (1981), Biophys. J. 34, 189–216
3 Bergelson, L.D. (1977) Methods Membrane Biol. 9, 275–335
4 Hutton, W.C., Yeagle, P.L. and Martin, R.B. (1977) Chem. Phys. Lipids 19, 255–265
5 Chrzeszczyk, A., Wishnia, A. and Springer, C.S. (1976) Am. Chem. Soc. Symp. 34, 483–498
6 Hauser, H., Hinckley, C.C., Krebs, J., Levine, B.A., Phillips, M.C. and Williams, R.J.P. (1977) Biochim. Biophys. Acta 468, 364–377
7 Manning, G.S. (1979) Acc. Chem. Res. 12, 443–449
8 Eisenberg, M., Gresalfi, T., Riccio, T. and McLaughlin, S. (1979) Biochemistry 18, 5 213–5 223
9 McLaughlin, A., Grathwohl, C. and McLaughlin, S. (1978) Biochim. Biophys. Acta 513, 338–357
10 Westman, J. and Eriksson, L.E.G. (1979) Biochim. Biophys. Acta 557, 62–78
11 Peppard, D.F., Mason, G.W. and Hucher, I. (1962) J. Inorg. Nucl. Chem. 24, 881–888
12 O'Brien, W.G. (1974) Ph.D. Dissertation, Iowa State University, Ames, IA
13 Zervas, L. and Dilaris, I. (1955) J. Am. Chem. Soc. 77, 5 354–5 357
14 Chen, P.S., Toribara, T.Y. and Warner, H. (1956) Anal. Chem. 28, 1 756–1 758
15 Chrzeszczyk, A., Wishnia, A. and Springer, C.S. (1977) Biochim. Biophys. Acta 470, 161–169
16 Wishnia, A. and Boussert, A. (1977) J. Mol. Biol. 116, 577–591
17 Spedding, F.H., Weber, H.O., Saeger, V.W., Petheram, H.H., Rard, J.A. and Habenschuss, A. (1976) J. Chem. Eng. Data 21, 341–360
18 Rard, J.A., Shiers, L.E., Heiser, D.J. and Spedding, F.H. (1977) J. Chem. Eng. Data 22, 337–347
19 Harned, H.S. and Owen, B.B. (1958) The Physical Chemistry of Electrolytic Solutions, 3rd edn., pp. 10, 59–88, 161, 165, 742, Reinhold Publishing Co., New York
20 Stewart, W.E. and Siddall, T.H. (1973) in Ion Exchange and Solvent Extraction, Vol. 3, (Marinsky, J.A. and Marcus, Y., eds.), pp. 83–110, Marcel Dekker, New York
21 Jesson, J.P. (1973) in NMR of Paramagnetic Molecules (LaMar, G.N., Horrocks, W.DeW. and Holm, R.H., eds.), Ch. 1, Academic Press, New York
22 Choppin, G.R. and Graffeo, A.J. (1965) Inorg. Chem. 4, 1 254–1 257
23 Choppin, G.R. (1971) Pure Appl. Chem. 27, 23–41
24 O'Brien, W.G. and Bautista, R.G. (1979) Adv. Chem. 177, 299–343
25 Choppin, G.R. and Strazik, W.F. (1965) Inorg. Chem. 4, 1 250–1 254
26 Hunt, G.R.A. and Tipping, L.R.H. (1980) J. Inorg. Biochem. 12, 17–36
27 McLaughlin, S. (1977) Curr. Topics Membranes, Transport 9, 71–144
28 Tanford, C. (1961) Physical Chemistry of Macromolecules, Ch. 7, John Wiley and Sons, Inc., New York
29 Grahame, D.C. (1947) Chem. Rev. 41, 441–501
30 Marshall, A.G. (1978) Biophysical Chemistry, pp. 81–84, John Wiley and Sons, New York
31 Hauser, H., Guyer, W., Levine, B., Skrabal, P. and Williams, R.J.P. (1978) Biochim. Biophys. Acta 508, 450–463
32 Brown, M.F. and Seelig, J. (1977) Nature 269, 721–723
33 Hauser, H., Phillips, M.C., Levine, B.A. and Williams, R.J.P. (1976) Nature 261, 390–394
34 Jain, M.K. and Wu, N.M. (1977) J. Membrane Biol. 34, 157–201
35 Hunt, G.R.A., Tipping, L.R.H. and Belmont, M.R. (1978) Biophys. Chem. 8, 341–355
36 Yeagle, P.L. (1978) Acc. Chem. Res. 11, 321–327
37 Skarjune, R. and Oldfield, E. (1979) Biochemistry 18, 5 903–5 909
38 Hauser, H., Guyer, W., Pascher, I., Skrabal, P. and Sundell, S. (1980) Biochemistry 19, 366–373
39 Barsukov, L.I., Shapiro, Yu.E., Viktorov, A.V., Volkova, V.I., Bystrov, V.F. and Bergelson, L.D. (1976) Bioorg. Khim. 2, 1 404 (English Translation, pp. 1 011–1 021)
40 Pearson, R.H. and Pascher, I. (1979) Nature 281, 499–501
41 Sears, B., Hutton, W.C. and Thompson, T.E. (1976) Biochemistry 15, 1 635–1 639
42 Michaelson, D.M., Horwitz, A.F. and Klein, M.P. (1973) Biochemistry 12, 2 637–2 645
43 Arnold, K. (1974) Studia Biophys. Berlin 42, 229–234
44 Copeland, B.R. and Anderson, H.C. (1981) J. Chem. Phys. 74, 2 548–2 558
45 Lichtenberg, D., Amselem, S. and Tamir, I. (1979) Biochemistry 18, 4 169–4 172
46 Barsukov, L.I., Victorov, A.V., Vasilenko, I.A., Evstigneeva, R.P. and Bergelson, L.D. (1980) Biochim. Biophys. Acta 598, 153–168
47 Cornell, B.A., Middlehurst, J. and Separovic, F. (1980) Biochim. Biophys. Acta 598, 405–410
48 Lin, G.S.B. and Macey, R.I. (1978) Biochim. Biophys. Acta 512, 270–283
49 Suurkuusk, J., Lentz, B.R., Barenholz, Y., Biltonen, R.L. and Thompson, T.E. (1976) Biochemistry 15, 1 393–1 401
50 Gruenewald, B., Stankowski, S. and Blume, A. (1979) FEBS Lett. 102, 227–229
51 Longmuir, K.J., Capaldi, R.A. and Dahlquist, F.W.

(1977) Biochemistry 16, 5 746–5 755
52 Hunt, G.R. and Tipping, L.R.H. (1978) Biochim. Biophys. Acta 507, 242–261
53 Eigenberg, K.E. and Chan, S.I. (1980) Biochim. Biophys. Acta 599, 330–335
54 Scott, H.L. and Cherng, S.-L. (1978) Biochim. Biophys. Acta 510, 209–215
55 Dill, K.A. and Flory, P.J. (1981) Proc. Natl. Acad. Sci. USA 78, 676–680
56 Blaurock, A.E. and Gamble, R.C. (1979) J. Membrane Biol. 50, 187–204
57 Lentz, B.R., Alford, D.R. and Dombrose, F.A. (1980) Biochemistry 19, 2 555–2 559
58 Gruen, D.W.R. and Haydon, D.A. (1980) Biophys. J. 30, 129–136
59 Israelachvili, J.N., Marcelja, S. and Horn, R.G. (1980) Q. Rev. Biophys. 13, 121–200
60 Eytan, G.D. and Broza, R. (1978) FEBS Lett. 85, 175–178
61 Lecompte, M.F., Miller, I.R., Elion, J. and Benarous, R. (1980) Biochemistry 19, 3 434–3 446
62 Wilschut, J.C., Regts, J., Westenberg, H. and Scherphof, G. (1978) Biochim. Biophys. Acta 508, 185–196
63 Machida, K. and Ohnishi, S.-I. (1980) Biochim. Biophys. Acta 596, 201–209
64 Miller, C., Arvan, P., Telford, J.N. and Racker, E. (1976) J. Membrane Biol. 30, 271–282
65 Akutsu, H. and Seelig, J. (1980) Abstracts of the Nineth International Conference on Magnetic Resonance in Biological Systems, p. 107